Covalent Ras dimerization on membrane surfaces through photosensitized oxidation

Jean K. Chung, Young Kwang Lee, Hiu Yue Monatrice Lam, Jay T. Groves

Supplementary Information

I. Materials

Fluorescent nucleotides ATTO488-GDP, ATTO488-GppNHp, ATTO594-GTP, and ATTO647N-GTP (Cat# NU-840-488, NU-860-488, NU-820-594, NU-820-647N) were purchased from Jena Biosciences (Jena, Germany). Lipids (1,2-di-(9Z-octadecenoyl)-*sn*-glycero-3-phosphocholine, DOPC; 1,2-dioleoyl-*sn*-glycero-3-phospho-*L*-serine, DOPS; 1,2-dioleoyl-*sn*-glycero-3-phosphoetahnolamine-N-[4-(p-maleimidomethyl)cyclohexane-carboxamide], MCC-DOPE) were purchased from Avanti Polar Lipids. Texas-Red DHPE (Cat# T-1395MP) was purchased from Life Technologies (now ThermoFisher Scientific, South San Francisco, CA). Ethylenediaminetetraacetic acid (EDTA), *L*-tyrosine, guanosine triphosphate (GDP), 5'-guanylyl imidodiphosphate (GppNHp), and other buffer components were purchased from Sigma-Aldrich (St. Louis, MO). Imaging buffer consisted of 2-mercaptoethanol (BME), glucose, Trolox, glucose oxidase, and catalase. All components were purchased from Sigma-Aldrich except glucose oxidase, which was purchased from Serva Electrophoresis GmbH (Heidelberg, Germany).

II. Methods

1. H-Ras purification.

A modified H-Ras with the following sequence was purified in the *E. coli* bacterial purification system reported in detail elsewhere:[1]

MTEYKLVVVG	AGGVGKSALT	IQLIQNHFVD	EYDPTIEDSY
RKQVVIDGET	CLLDILDTAG	QEE**Y**SAMRDQ	YMRTGEGFLC
VFAINNTKSF	EDIHQYREQI	KRVKDSDDVP	MVLVGNKSDL
AARTVESRQA	QDLARSYGIP	YIETSAKTRQ	GVEDAFYTLV
REIRQHKLRK	LNPPDESGPG	C	

The terminal cysteine serves as the reaction site to bind the protein to the bilayer. The underlined Y denotes the location of the Y64A mutation. His-6 construct contained six histidine residues at the C-terminus.

2. Sample preparations for Ras on supported lipid bilayers.

Membrane-bound H-Ras samples were prepared for FCS and SPT experiments. Relevant protocols have been reported in detail previously.[2] Briefly, supported lipid bilayer was formed by

rupture of small unilamellar vesicles (SUVs), prepared by extrusion, on glass substrates cleaned by piranha etch. A typical batch of SUVs were prepared in the following lipid composition: 2% MCC-DOPE, 2% DOPS, 96% DOPC and a trace amount (0.0025 – 0.01%) of Texas Red-DHPE. The bilayers were prepared in ibidi sticky-Slide VI 0.4 chambers (ibidi GmbH, Martinsried, Germany) for imaging. H-Ras was tethered to the bilayer via thiol-maleimide conjugation between the terminal cysteine (C181) and maleimide in the headgroup of MCC-DOPE lipids. Native nucleotide cofactors were exchanged for ATTO488-labeled guanosine nucleotides after being stripped with 50 mM EDTA. The final sample was in 50 mM HEPES, 150 mM NaCl, and 5 mM $MgCl_2$. The imaging buffer was of the following composition: 10 mM BME, 20 mM glucose, 2 mM UV-treated Trolox, 320 μg/mL glucose oxidase, and 50 μg/mL catalase in the HEPES buffer.[3-5]

3. Ras crosslinking reactions in solution.

Laser irradiation. Cys181 residue in H-Ras was capped with 10-fold molar excess maleimide for 30 min at room temperature to avoid potential disulfide cross-linking. Endogenous nucleotides in Ras were exchanged with desired fluorescent or dark GDP before light illumination. In a typical exchange reaction, Ras was incubated with 25 mM EDTA in 50 mM HEPES/150 mM NaCl buffer for at 4 °C for 30 min to chelate Mg^{2+} which is a cofactor for guanine nucleotide binding. EDTA and released endogenous nucleotide were removed by buffer exchange with 50 mM HEPES/150 mM NaCl using size exclusion spin column (Bio-Rad). A two-fold molar excess of desired nucleotides with respect to Ras was incubated overnight at 4 °C in the presence of 5 mM of Mg^{2+}. Ras concentration was adjusted to be 1 mg/ml for light illumination experiments. For free tyrosine experiments, 0.1 mM L-tyrosine (Sigma-Aldrich) and 10 μM Alexa Fluor 488 (Life Technologies) in HEPES buffer was illuminated using identical conditions.

UV irradiation. H-Ras labeled with dark GDP were illuminated with 306-nm-UV light for 60 min. To avoid heating the solution, illumination was paused every 10 min and the solution was cooled down in an ice bath for 10 min.

HRP-peroxide crosslinking. Enzymatic oxidative reactions were catalyzed by horseradish peroxidase (HRP) in the presence of hydrogen peroxide as the oxidizing agent. HRP has a similar molecular weight to H-Ras dimer, and thus appears overlapped with H-Ras dimer in the SDS-PAGE gel. This could be an issue to detect H-Ras dimer. In order to circumvent this issue, we used HRP-magnetic microparticle complexes, and completely removed HRP after enzymatic reactions using magnetic separator (Invitrogen). 10 μL of HRP stock solution (Invitrogen) was incubated with 0.5 mg of magnetic particles (Promega) for 30 min to physically adsorbed HRP on the particle surfaces. Unbound HRP was removed by washing three times with PBS followed by an additional washing with 50 mM HEPES/100 mM NaCl/5 mM $MgCl_2$. 50 μL of 1 mg/mL H-Ras was reacted with 0.1 mg of HRP-magnetic particle complexes in the presence of 10 mM of H_2O_2 for 30 min. After reaction, supernatant containing H-Ras was collected after HRP-magnetic particle complexes were removed by magnetic separation. The supernatant was centrifuged at 1500 g for 5 min to remove residual particles. The top layer was carefully collected and loaded into gel electrophoresis.

4. SDS-PAGE Gel Electrophoresis

The precast polyacrylamide gels used in the study were NuPAGE Novex 4-12% Bis-Tris protein gels (Life Technologies). Running buffer was prepared from 1M Tris base, 1M 2-(*N*-morpholino)ethanesulfonic acid (MES), 20.5mM EDTA and 2% sodium dodecyl sulfate (SDS). Ras proteins diluted to 1 mg/mL, as confirmed using NanoDrop 2000 (Thermo Scientific), were mixed with lithium dodecyl sulfate sample buffer (Life Technologies) and and MilliQ water at a ratio of 2:1:1. The samples were heated at 95^{o}C for 3 min on a heat block before they were loaded into individual wells. The electrophoresis process was set at 200 V, 400 mA. The gels were subsequently transferred to a plastic container with DI water, and stained with Sypro Ruby protein gel stain (Molecular Probes) using the rapid staining protocol. The gels were imaged using a benchtop 2UV transilluminator at 302 nm.

5. Fluorescence Correlation Spectroscopy

Dual-color FCS was performed on a home-built setup with a modified inverted microscope (Nikon TE2000). For excitation, wavelengths selected by bandpass filters from a pulsed white light laser source (SuperK Extreme EXW-12, NKT Photonics, Copenhagen, Denmark) were used. The excitation pulses are sent into a single mode optical fiber, then the combined pulses enter the microscope via a multi-color dichroic cube (Di01-R405/488/561/635-25x36, Semrock). Notch filters were used to remove excess excitation intensity. The fluorescence signal is collected by the 100x high-NA oil immersion objective, and recorded by avalanche photodiode detectors (Hamamatsu). The signal is directly converted into autocorrelation signal by a hardware correlator (Correlator.com). In the experiments described in the text, blue light (488 nm) was used to excite the ATTO 488 fluorophore, and orange light (568 nm) for exciting Texas Red-DHPE simultaneously. The average power used to excite the sample ranged between 0.5 and 5.0 μW depending on the fluorophore quantum yield and the surface density, which is equivalent to the irradiance range of 0.4 ~ 4.0 kW/cm^2 calculated with the calibrated spot sizes. The resulting autocorrelation G(τ) was fit to the two-dimensional Gaussian diffusion model,

$$\mathrm{G}(\tau) = \frac{1}{N}\left(\frac{1}{1+\tau/\tau_D}\right)$$

Where τ is time delay, N is the number of particles in the focus spot, τ_D is the correlation time. To calibrate the spot size of the confocal focus, N of a bilayer with a known surface density of fluorescent lipids of each color, BODIPY-FL-DHPE (Life Technologies) for 488 nm and Texas Red-DHPE for 568 nm, were measured, which consistently yielded the radius of 0.20 ± 0.01 μm and 0.22 ± 0.01 μm for 488 nm and 568 nm, respectively. The diffusion coefficient D was calculated by using the relation

$$D = w^2/4\tau_D$$

Where w is the radius of the focus spot size.

6. Single Particle Tracking

Single-molecule imaging experiments were performed on a Nikon eclipse Ti inverted microscope with a 100× 1.49 N.A. oil immersion TIRF objective and iXon EMCCD camera (Andor Technology Ltd., UK). 640-nm (RCL-050-640, Crystalaser, NV), 561-nm (Sapphire HP, Coherent Inc., CA) and 488-nm (Sapphire SF, Coherent Inc., CA) were used as illumination sources

for TIRF imaging. A dark background before single-molecule imaging was achieved typically by a 20-s photobleaching with the laser power of 20 mW at the objective. Single-molecule data were quantified using an ImageJ plugin (TrackMate)[6] and analyzed in Igor Pro (WaveMetrics). The step size distribution for each sample was fit with both the single- and two-component Brownian diffusion model. The probability density for a particle with diffusion coefficient (D) to move a distance (r) in time interval (t) is

$$p(r,t,D) = \frac{r}{2Dt}\exp\left(-\frac{r^2}{4Dt}\right).$$

Therefore, two-component diffusion with two different diffusion coefficients (D_1 and D_2) and the relative population for the first component (α) is described by the following equation:

$$p(r,t,D) = \frac{\alpha r}{2D_1 t}\exp\left(-\frac{r^2}{4D_1 t}\right) + \frac{(1-\alpha)r}{2D_2 t}\exp\left(-\frac{r^2}{4D_2 t}\right).$$

Fitting residues for the single- and two-component model were monitored to determine the number of diffusion species. The diffusion coefficients and relative population of each component were calculated from the corresponding fitting.

III. Supplementary Figures and Table

Figure S1

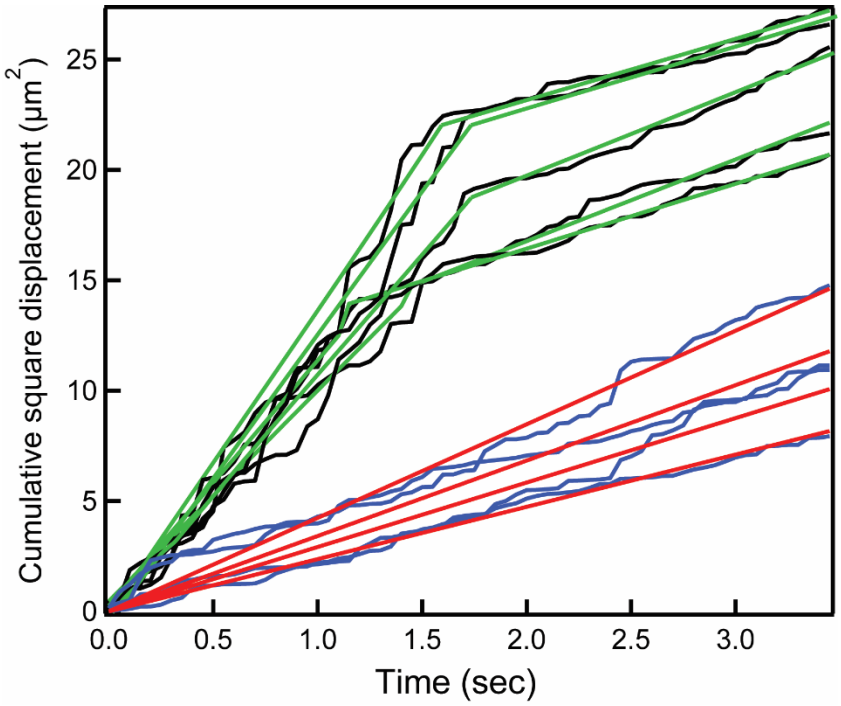

Figure S1. Long trajectories of Ras on SLB by SPT. Cumulative square displacement plots (CSD) of individual wild type H-Ras trajectories (blue line). The plots well agree with linear fitting (red line), showing Ras stay in a single diffusion state until they bleach out. Simulated trajectories undergoing diffusion coefficient change from 3 to 0.7 $\mu m^2/s$ exhibit change points of diffusion sate (black line: CSD of simulated trajectories; green line: linear fitting of CSD). Change points were detected by Bayesian detection model.

Figure S2

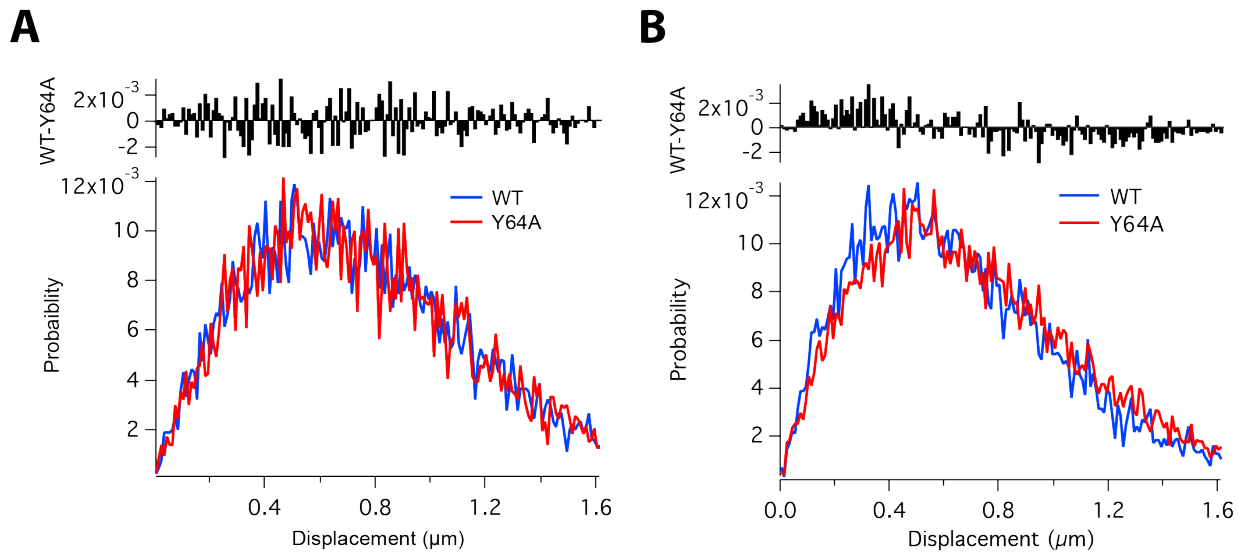

Figure S2. Comparison of step size distributions between WT and Y64A mutant Ras. Step size distributions were collected by SPT for WT and Y64A mutant Ras at similar densities: (A) 220/μm^2 and 230/μm^2 for WT and Y64 mutant Ras, respectively, and (B) 1100/μm^2 and 1150/μm^2. Differences between WT and Y64 step size distributions are plotted in the top inset for each density. At a low density, WT and Y64A Ras show identical diffusion on membranes. However, WT Ras diffuse more slowly with respect to Y64A at a higher density, which is characterized by systematic variations of displacement between two constructs, indicating that WT construct undergoes greater extent of oxidative crosslinking compared to Y64A.

Figure S3

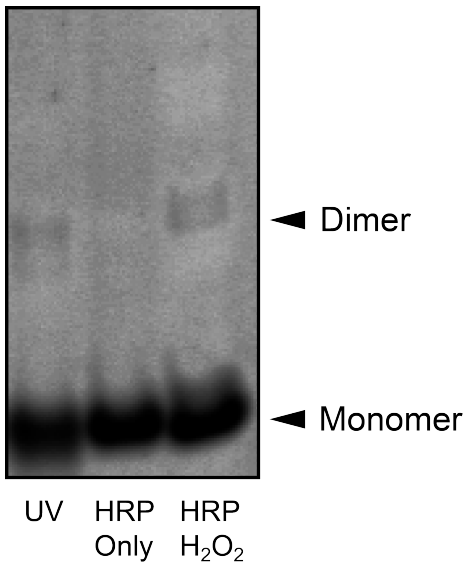

Figure S3. SDS-PAGE Gel Electrophoresis of Ras subjected to various oxidative stresses. H-Ras forms covalent dimers under the UV illumination and enzymatic oxidative stress. For UV exposure, 306-nm-UV light illuminated H-Ras for 60 min. Enzymatic oxidative reactions were catalyzed by horseradish peroxidase conjugated on magnetic particles in the presence of 10 mM of hydrogen peroxide as the oxidizing agent for 30 min. After reaction, HRP was removed by magnetic separation. Covalent Ras dimers were formed only when hydrogen peroxide is present, which indicates that the band appears in dimer molecular weight is oxidative product but not HRP (44 kDa). See **SI Methods** for details on sample preparations and experiment.

Figure S4

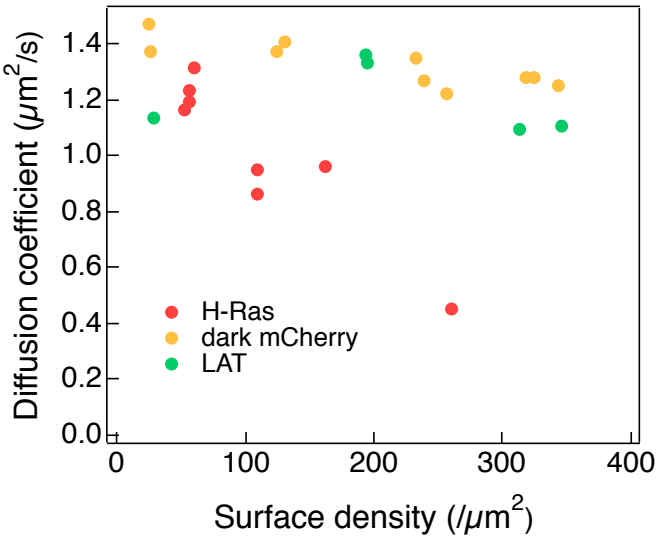

Figure S4. Density-dependent FCS for various proteins. Density-dependent diffusion coefficient of H-Ras-His_6:ATTO488-GDP, dark mCherry-His_{10}-Alexa Fluor 488, and LAT-His_6-Alexa Fluor 555 measured by FCS. The dark mCherry has a Y67S point mutation, which renders the protein nonfluorescent.[7] For LAT, the human LAT cytosolic domain (residues 30 to 233) was expressed and purified using the *E. coli* bacterial system.[8] Dark mCherry and LAT were labeled with Alexa Fluor 488 and Alexa Fluor 555 (Life Technologies), respectively, by cysteine-maleimide labeling reaction. The proteins were coupled to the bilayer (4% Ni-NTA-DOGS, 96% DOPC) by Histidine tag-nickel chelation method.[9,10]

Table S1

	PDB ID	Tyr	His	Trp	Cys	Surface area (Å^2)
H-Ras	4EFL	9	4	0	1	7662
Rac1	3TH5	4	2	1	2	7413
RhoA	1FTN	3	2	1	0	8106
Rab1A	2FOL	7	1	2	1	7160
Rap1A	3ZFI	0	4	0	0	8073
mCherry	2H5Q	4	5	0	0	9226

Table S1. Comparison of the number of oxidation-sensitive amino acid residues exposed on the surface for various GTPases and mCherry. Crystal structure was analyzed using UCSF Chimera. Chimera is developed by the Resource for Biocomputing, Visualization, and Informatics at the University of California, San Francisco (supported by NIGMS P41-GM103311).[11]

SI References

(1) Gureasko, J.; Galush, W. J.; Boykevisch, S.; Sondermann, H.; Bar-Sagi, D.; Groves, J. T.; Kuriyan, J. *Nat. Struct. Mol. Biol.* **2008**, *15*, 452.
(2) Lin, W. C.; Iversen, L.; Tu, H. L.; Rhodes, C.; Christensen, S. M.; Iwig, J. S.; Hansen, S. D.; Huang, W. Y. C.; Groves, J. T. *P. Natl. Acad. Sci. U.S.A.* **2014**, *111*, 2996.
(3) Rasnik, I.; McKinney, S. A.; Ha, T. *Nat. Methods* **2006**, *3*, 891.
(4) Cordes, T.; Vogelsang, J.; Tinnefeld, P. *J. Am. Chem. Soc.* **2009**, *131*, 5018.
(5) Aitken, C. E.; Marshall, R. A.; Puglisi, J. D. *Biophys. J.* **2008**, *94*, 1826.
(6) Jaqaman, K.; Loerke, D.; Mettlen, M.; Kuwata, H.; Grinstein, S.; Schmid, S. L.; Danuser, G. *Nat. Methods* **2008**, *5*, 695.
(7) Fourniol, F. J.; Li, T. D.; Bieling, P.; Mullins, R. D.; Fletcher, D. A.; Surrey, T. *Methods Enzymol.* **2014**, *540*, 339.
(8) Yan, Q.; Barros, T.; Visperas, P. R.; Deindl, S.; Kadlecek, T. A.; Weiss, A.; Kuriyan, J. *Mol. Cell. Biol.* **2013**, *33*, 2188.
(9) Lin, W. C.; Yu, C. H.; Triffo, S.; Groves, J. T. *Curr. Protoc. Chem. Biol.* **2010**, *2*, 235.
(10) Nye, J. A.; Groves, J. T. *Langmuir* **2008**, *24*, 4145.
(11) Pettersen, E. F.; Goddard, T. D.; Huang, C. C.; Couch, G. S.; Greenblatt, D. M.; Meng, E. C.; Ferrin, T. E. *J. Comput. Chem.* **2004**, *25*, 1605.